Tomographic Microwave Diversity Image Reconstruction Employing Unitary Compression

Zijun Zhao, *Member, IEEE,* and Nabil H. Farhat, *Fellow, IEEE*

Abstract—**Data compression through a unitary transform is utilized in tomographic microwave diversity image reconstruction in order to reduce the dimensionality and to extract the features in the data space. The unitary compression is derived by minimizing the mean-square error (MSE) and the unitary transform is made of eigenvectors of the data's covariance, regarded to be a Karhunen–Loéve transform. Tomographic microwave frequency-swept imaging was developed using a unique target-derived reference technique to access the three dimensional Fourier space of the scatterer and an image reconstruction algorithm based on the projection slice theorem. It is shown that: centimeter resolution of a complex object can be preserved even when half of the data set is compressed; and that the reconstructed image remains identifiable by a human observer even when 2/3 of the data set is compressed.**

I. Introduction

TOMOGRAPHIC microwave diversity imaging was developed and has been in use at the Electro-Optics & Microwave-Optics Laboratory at the University of Pennsylvania for over a decade. It demonstrates the feasibility of broad-band projective imaging, with near-optical resolution, of complex shaped scattering object in the 2–26.5 GHz range [1]–[4]. The basic working principle of tomographic microwave diversity imaging relies on the Bojarski identity of inverse scattering theory [7], [8]. Based on this principle one can access a 2-D slice of the 3-D Fourier space of the scattering object by measuring the scattered field from an object that can be rotated in azimuth relative to a fixed broad-band transmitter/receiver (T/R) assembly and by digitally sweeping the transmitted signal over a bandwidth of several GHz for each rotation angle and coherently detecting the backscattered wave field. The Fourier space data acquired in this fashion, is made of frequency response echos which are measured at different aspect views of the object which are equally spaced over a prescribed angular window. Each echo is quantized over the sweeping frequency spectrum. If these frequency response echos are considered as samples of a stochastic process, they are mutually correlated and have some redundancy.

Manuscript received November 21, 1990; revised August 8, 1991. This work was supported by the Army Research Office and the SDIO/IST.

The authors are with the Electro-Optics & Microwave-Optics Laboratory, The Moore School of Electrical Engineering, University of Pennsylvania, Philadelphia, PA 19104.

IEEE Log Number 9105264.

In the practical applications of tomographic microwave diversity imaging, there is an emerging problem of how to deal with the vast amount of 2-D data acquired from an imaging radar. For instance, target identification methods that form an associative memory based on neural networks [4] require that the data set be reduced. Similar problems appear in telecommunication and communication networks where the capacity of the transmission channel is limited and signal (data/image/voice) to be transmitted have to be compressed before the transmission in order to achieve fast and least distorted transmission. For all these data compression problems, the key point is how to find a signal representation identifying the redundancy of the signal to be compressed. Although no representation is best in all senses, the unitary transform has been widely used to serve as one of the signal representation in a lot of applications such as image processing [5], speech processing [6], feature selection in pattern recognition [17], and analysis and design of communication systems [11]. Unitary compression is a technique that applies the unitary transform to data compression, which allows the redundancy of the data to be identified and thus removed. The procedure of applying the unitary transform to the data compression is described as follows: the measured Fourier data is unitarily transformed to a domain in which coordinates are de-correlated, and redundant ones are identified and removed; the new Fourier space data is then obtained by the inverse unitary transform while maintaining a tolerable fixed distortion.

Based on the criterion of minimizing the mean-square error, a unitary transform, called Karhunen–Loéve transform (KLT), can be given, which will make the vectors in the data space orthogonal with respect to each other. As pointed out by Watanaba [13], the Karhunen-Loéve expansion enables the extraction from a given set of data those features which are the most significant, i.e., which bear the greatest amount of information. To do this one works with the covariance matrix averaged over the whole data set and diagonalizes it. The data features are then the eigenvectors and the dominance or importance of these features are the eigenvalues. While a subset of the data with respect to smaller eigenvalues of the data's covariance matrix is defined as redundant ones, the mean-square error, which is derived as a summation of eigenvalues of the covariance, will be minimized. The Karhunen–Loéve expansion has been widely used as a signal representation to derive optimal receivers in communication, radar and sonar applications because it involves bi-orthogonality, i.e., that both bases and coefficients are orthogonal (or unitary for complex process) [11], [12].

In this paper, we present first a brief review of the principle of broad-band projective imaging by wavelength diversity, along with a description of the procedure we used to access the Fourier space of scattering objects, employing our experimental microwave imaging facility. The next part will be a simple introduction to the KLT and its properties. The main part of the paper will describe image reconstruction employing unitary compression technique. This section presents both theoretic derivation and experimental results of the reconstructed images, as well as a discussion of the implication of these results.

II. Tomographic Microwave Diversity Imaging

It is well-known that under physical optics approximation, the scattered field for a perfectly conducting object due to plane wave illumination is given by [3]:

$$\psi(\boldsymbol{p}, R) = \frac{jAke^{-jkR}}{2\pi R} \int_{-\infty}^{\infty} \gamma(\boldsymbol{r}) e^{j\boldsymbol{p} \cdot \boldsymbol{r}} \, d\boldsymbol{r} \tag{1}$$

where $\gamma(\boldsymbol{r})$ represents scattering characteristic function of the object; $\boldsymbol{r}$ is a position vector of an object point measured relative to a common origin in the object; R is the distance between an observation point and the common origin; A represents the strength of the incident illumination, and $\boldsymbol{p}$ is a position vector in Fourier space that is expressed as

$$\boldsymbol{p} = k(\bar{\boldsymbol{l}}_R - \bar{\boldsymbol{l}}_i) \tag{2}$$

where $\bar{\boldsymbol{l}}_R$ is the unit vector in the direction of the observation point and $\bar{\boldsymbol{l}}_i$ the incident unit vector. It is obvious that $\psi(\boldsymbol{p}, R)$ can be regarded as a generalized (3-D) Fourier transform hologram of the scattering function of the object multiplied by a complex constant. The diversity of microwave imaging stems from varying by $\bar{\boldsymbol{l}}_R$ and/or $\bar{\boldsymbol{l}}_i$ (angular diversity) and sweeping k (frequency diversity).

Automated measurement of the scattered field from any band in the 2–26.5 GHz frequency range is provided by a coherent microwave measurement system consisting of a microwave sweeper and a coherent receiver shown in Fig. 1. The test object, a metallized 100 : 1 scale model of a B-52 aircraft with a 79-cm wing span and 68-cm fuselage, was mounted on a computer-controlled positioner situated in an anechoic chamber. The measurement sequence consisted of angular rotation in azimuth with 0.7 degree increment, frequency stepping in any band from 2–26.5 GHz in selected frequency steps, and measurement and storage of the amplitude and phase from the coherent receiver, as well as correction of clutter and system response. All measurements ware carried out under control of a DEC modulator instrumentation computer (MINC 11/2). To avoid aliasing in image space, the frequency steps were selected in increments of $\delta f = c/2L$, where L is the characteristic size of the scattering object. Assuming $L = 79$ cm for the model B-52, a $\delta f = 74.6$ MHz was used; thus 201 frequency steps were needed to cover the 2–17 GHz range in order to satisfy the Nyquist sampling criterion. The azimuth angle ϕ was changed from 0 degree to 90 degrees in steps of 0.7 degree for a total of 128 angular looks extending from the head-on to the broadside orientation of the B-52.

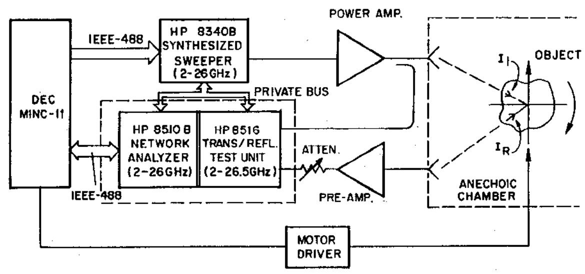

Fig. 1. Tomographic microwave diversity imaging system scheme.

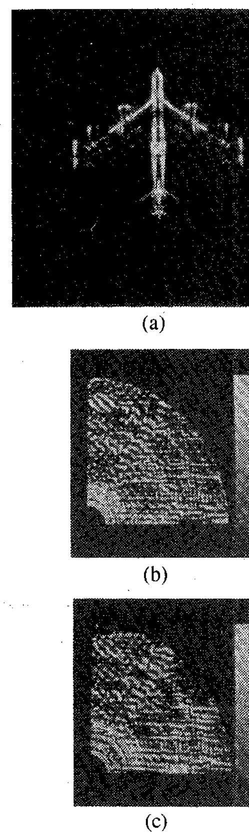

Fig. 2. Results of tomographic microwave imaging of a 100 : 1 scale model of the B-52 airplane for frequency-swept range 2–17 GHz and angular diversity 90° covered by 128 views. (a) Projection image. (b) Real part of Fourier space slice taken. (c) Imaginary part of Fourier space slice taken.

Examples of a slice of the 3-D Fourier domain of the B-52 are shown in Fig. 2(b) and (c) which consist of polar plots of 201 frequency points. In these polar plots frequency is along the radial direction and aspect (azimuth angle) is in the angular direction. Fourier inversion of the slice data should yield a projection image of the scattering centers of the target on a plane normal to the azimuthal axis of the rotation, i.e., the shape estimation of the object shown in Fig. 2(a). Resolution of the reconstructed image is estimated to be about 2 cm from observed details such as the engines and tail section in this image.

III. Karhunen–Loéve Transform

The unitary transforms, defined in a linear inner-product space in a complex field which is also called unitary space, are of complex forms of the orthogonal transforms. The Karhunen–Loéve transform is one of them and will be outlined for review and to provide background for the notation used in this paper. It is assumed that a given X is a second-order discrete stochastic process and that its covariance is denoted by a 2-D matrix Σ_x defined by

$$\Sigma_x = E[(\boldsymbol{x} - \boldsymbol{m}_x)(\boldsymbol{x} - \boldsymbol{m}_x)^*] \tag{3}$$

where $E[\cdot]$ denotes the statistical expectation; $\boldsymbol{m}_x$ is the 1-D mean vector of X; and $*$ is complex transpose. Since X is a complex process, Σ_x is Hermitian (i.e., complex conjugate with real diagonal elements). We are interested only in the truncated version of the Karhunen–Loéve transform because it has been shown [12] to yield the best approximation of a stochastic process of all N-dimensional approximations.

Let $T^* = [\phi_1, \cdots, \phi_N]$ be a complete, unitary basis such that X can be expanded in the sense of the mean-square convergence:

$$X \doteq \sum_{i=1}^{N} \boldsymbol{y}^{(i)} \phi_i \tag{4}$$

where $\boldsymbol{y}^{(i)}$ are coordinates vector, and the notation $\doteq$ represents the mean-square equivalence, i.e.,

$$E\left[\left(X - \sum_{i=i}^{N} \boldsymbol{y}^{(i)} \phi_i\right)^2\right] = 0. \tag{5}$$

Owing to the unitary characteristics of the basis vector T, the coordinates $\boldsymbol{y}^{(i)}$ can be obtained by

$$\boldsymbol{y}^{(i)} = \langle X, \phi_i \rangle \tag{6}$$

where $\langle \cdot, \cdot \rangle$ denotes a complex inner-product for the discrete case. The expansion given by (4) is regarded as the Karhunen–Loéve expansion when the basis vector T is chosen such that the coordinates are unitary in the probabilistic sense:

$$E[(\boldsymbol{y}^{(i)} - \boldsymbol{m}_y^{(i)})(\boldsymbol{y}^{(j)} - \boldsymbol{m}_y^{(j)})^*] = \lambda_i \delta_{ij} \tag{7}$$

where δ_{ij} is the Kronecker delta function; λ_i, an eigenvalue of X's covariance, is given by

$$\Sigma_x \phi_i = \lambda_i \phi_i \tag{8}$$

where Σ_x is a Hermitian and non-negative definite matrix, and ϕ_i are eigenvectors of Σ_x. The Karhunen–Loéve transform is therefore considered a bi-unitary transform because both the coordinates and the basis vectors are unitary. It is shown that the Karhunen–Loéve transform is made of the eigenvectors of the data's covariance.

If we denote $Y^* = [\boldsymbol{y}^{(1)}, \cdots, \boldsymbol{y}^{(N)}]$, then (4) can be expressed in matrix format:

$$X = T^* Y \tag{9}$$

Since $\{\phi_i, i = 1, \cdots, N\}$ are unitary with respect to each other, i.e.,

$$\phi_i \phi_j = \begin{cases} 1 & i = j \\ 0 & i \neq j \end{cases}, \tag{10}$$

then

$$TT^* = I, \tag{11}$$

where I is the identity matrix, and (11) can be rewritten by

$$T^{-1} = T^*. \tag{12}$$

Hence, the inverse of a unitary matrix is the complex transpose of the matrix. (9) can, therefore, be rewritten by multiplying T using (11)

$$Y = TX. \tag{13}$$

The covariance of Y is then given by

$$\Sigma_y = T\Sigma_x T^{-1} = T\Sigma_x T^*. \tag{14}$$

From linear algebra, it is known that a Hermitian matrix can be diagonalized by a unitary matrix consisting of eigenvectors of the Hermitian matrix, with the eigenvalues of the Hermitian matrix as its diagonal elements [14]. Since the covariance matrix Σ_x is Hermitian and T is consisting of eigenvectors of the matrix Σ_x, the covariance matrix Σ_y given by (14) can be diagonalized with the eigenvalues of Σ_x as its diagonal elements. Thus, (14) can be rewritten by

$$\begin{aligned} \Sigma_y &= T\Sigma_x T^{-1} \\ &= T\Sigma_x T^* \\ &= \begin{bmatrix} \lambda_1 & & \\ & \ddots & \\ & & \lambda_N \end{bmatrix}. \end{aligned} \tag{15}$$

This result implies that the coordinates matrix Y is unitary because its covariance matrix is diagonal. Since the unitary transform is an inner-product invariant, norm invariant transform, the variance is not changed after the Karhunen–Loéve transform. The variance of X can be expressed by the diagonal terms of Y

$$\begin{aligned} Var(X) &= Var(Y) \\ &= \sum_{i=1}^{N} \lambda_i \end{aligned} \tag{16}$$

where λ_i are the eigenvalues of Σ_x.

IV. Image Reconstruction Employing Unitary Compression

A. Theoretical Foundation

The image reconstructed from a sufficient quantity of acquired Fourier space data is displayed in Fig. 2. However, the acquired Fourier space data is correlated and there exists redundancy in terms of correlation. The unitary compression is a technique in which the mean-square error due to eliminating the redundant data is minimized through a unitary transform. This unitary transform allows us to extract the most significant features of the acquired data and to compress the data sets so that their redundancy can be removed. The procedure of applying the unitary transform to the image reconstruction or image transmission is depicted in Fig. 3. The Fourier space data X is unitarily transformed to a domain in which coordinates $y^{(i)}$ are de-correlated, and redundant ones are identified and removed. The new Fourier space data $\hat{X}$ is obtained by the inverse unitary transform T^{-1} while maintaining a tolerable fixed distortion between X and $\hat{X}$. Thus, $\hat{X}$ is considered an effective representation containing the most significant information and is used to reconstruct images.

According to Fig. 3, for the acquired data vector X, we obtain

$$Y = TX; \tag{17}$$

where

$$X^* = [x^{(1)}, \cdots, x^{(N)}];$$
$$Y^* = [y^{(1)}, \cdots, y^{(N)}];$$

and

$$T^* = [\psi_1, \cdots, \psi_N].$$

From (17) and it follows that $TT^* = I$, and hence

$$X = T^*Y = \sum_{i=1}^{N} y^{(i)}\psi_i. \tag{18}$$

where X can be referred to as an expansion in terms of a complete unitary bases $\psi_i (i = 1, \cdots, N)$ and $y^{(i)}$ are the coordinates. If we wish to retain a subset $\{y^{(1)}, \cdots, y^{(M)}\}$ of Y (M $\leq$ N) and yet estimate X. This can be done by replacing remaining $N - M$ components of Y by preselected constants vector $b^{(i)}$ $(i = M + 1, \cdots, N)$ to obtain

$$\hat{X} = \sum_{i=1}^{M} y^{(i)}\psi_i + \sum_{i=M+1}^{N} b^{(i)}\psi_i. \tag{19}$$

where $\hat{X}$ denotes the estimate of X. The error ΔX introduced by neglecting the $N - M$ terms can be represented

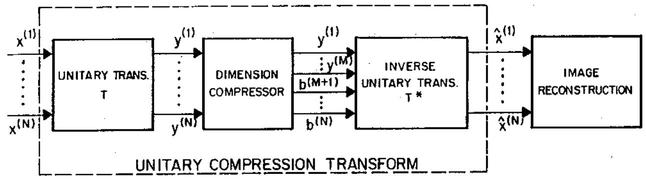

Fig. 3. Block diagram of the image reconstruction procedure with unitary compression transform.

as

$$\begin{aligned}\Delta X &= X - \tilde{X} \\ &= X - \sum_{i=1}^{M} y^{(i)}\psi_i - \sum_{i=M+1}^{N} b^{(i)}\psi_i \\ &= \sum_{i=1}^{N} y^{(i)}\psi_i - \sum_{i=1}^{M} y^{(i)}\psi_i - \sum_{i=M+1}^{N} b^{(i)}\psi_i \\ &= \sum_{i=M+1}^{N} (y^{(i)} - b^{(i)}\psi_i.\end{aligned} \tag{20}$$

Thus the mean-square error ϵ is given by

$$\epsilon = E[\|\Delta X\|^2] = E[\Delta X \cdot \Delta X^*] \tag{21}$$

where $\|\cdot\|$ is a norm notation. Substitution of (20) in (21) leads to

$$\begin{aligned}\epsilon &= E\left[\sum_{i=M+1}^{N}\sum_{j=M+1}^{N} (y^{(i)} - b^{(i)})(y^{(i)} - b^{(i)})^*\psi_i\psi_j^*\right] \\ &= \sum_{i=M+1}^{N} E[(y^{(i)} - b^{(i)})^2];\end{aligned} \tag{22}$$

where the unitary property of ψ_i is used to simplify the result in (22). In order to minimize the ϵ by choosing both $b^{(i)}$ and ψ_i, we take the derivatives of ϵ with respect to $b^{(i)}$ and ψ_i and set them to zero, that is

$$\frac{\partial \epsilon}{\partial b^{(i)}} = -2\{E[y^{(i)}] - b^{(i)}\} = 0 \tag{23}$$

which yields

$$\begin{aligned}b^{(i)} &= E[y^{(i)}] \\ &= m_y^{(i)} \\ &= \psi_i^* m_x^{(i)}\end{aligned} \tag{24}$$

where $m_x^{(i)}$ and $m_y^{(i)}$ represents the means of X and Y, respectively. Hence, the mean-square error ϵ can be rewritten after substituting (24) into (22):

$$\begin{aligned}\epsilon &= \sum_{i=M+1}^{N} \psi_i E[(x - m_x)(x - m_x)^*]\psi_i^* \\ &= \sum_{i=M+1}^{N} \psi_i^* \Sigma_x \psi_i;\end{aligned} \tag{25}$$

where

$$\Sigma_x = E[(x - m_x)(x - m_x)^*]$$

is the covariance matrix of X.

To obtain the optimal $\psi_i (i = 1, \cdots, N)$ we must not only minimize ϵ with respect to ψ_i, but also satisfy the unitary constraint:

$$\psi_i \psi_j = \delta_{ij};$$

or

$$TT^* = I.$$

Thus we use the method of Lagrange multipliers and minimize

$$\tilde{\epsilon} = \epsilon - \sum_{i=M+1}^{N} \theta_i [\psi_i^* \psi_i - 1]$$

$$= \sum_{i=M+1}^{N} \psi_i^* \Sigma_x \psi_i - \theta_i [\psi_i^* \psi_i - 1]; \quad (26)$$

with respect to ψ_i, where θ_i denotes the Lagrange multiplier. By taking the derivatives with respect to ψ_i, we have

$$\frac{\partial \epsilon}{\partial \psi_i} = \nabla_{\psi_i} [\psi_i^* \Sigma_x \psi_i] - 2\theta_i \nabla_{\psi_i} [\psi_i^* \psi_i] \quad (27)$$

where ∇ denotes a vector derivative operator. The following can be given from the differentiability of the matrix:

$$\nabla_{\psi_i} [\psi_i^* \Sigma_x \psi_i] = 2\Sigma_x \psi_i; \quad (28)$$

and

$$\nabla_{\psi_i} [\psi_i^* \psi_i] = 2\psi_i. \quad (29)$$

Thus, from (27) we have

$$\frac{\partial \epsilon}{\partial \psi_i} = 2\Sigma_x \psi_i - 2\theta_i \psi_i = 0; \quad (30)$$

which yields

$$\Sigma_x \psi_i = \theta_i \psi_i, \quad (31)$$

in which ψ_i are the eigenvectors of the covariance matrix Σ_x, i.e., $\psi_i = \phi_i (i = 1, \cdots, N)$, and θ_i are the eigenvalues, i.e., $\theta_i = \lambda_i (i = 1, \cdots, N)$. As previously discussed, the unitary transform T, consisting of eigenvectors of the covariance matrix, is called Karhunen–Loéve transform. It has been shown that Y is unitary (i.e., uncorrelated), which makes it useful in identification where the unique features of the data can be extracted from the unitary data sets based on *Principal Component Analysis* [17] in which the redundancy of the data can be discerned [18]. The mean-square error can be given by substituting (31) in (25):

$$\epsilon = \sum_{i=M+1}^{N} \phi_i^* (\lambda_i \phi_i)$$

$$= \sum_{i=M+1}^{N} \lambda_i. \quad (32)$$

The mean-square error caused by discarding the $N - M$ redundant vectors is the summation of the $N - M$ eigenvalues of the covariance matrix Σ_x. This result indicate that the effectiveness of a transform component $y^{(i)}$ for representing the data vector X, is determined by its corresponding eigenvalue. If a component $y^{(i)}$ is deleted, then the mean-square error increases by λ_i, the corresponding eigenvalue. Thus the set of $y^{(i)}$ with the M largest eigenvalues should be selected, and the remaining $y^{(i)}$ discarded since they can be replaced by the constants $b^{(i)}$, $i = M + 1, \cdots, N$. It is, therefore, obvious that in order to minimize the mean-square error while maximizing the possibility of compressing the data (i.e., maximizing M), the vectors chosen to be discarded should be these with smaller eigenvalues. Based on the above analysis, two important conclusions are given as follows: 1) The KLT is the optimal transform for unitary compression with respect to the mean-square error criterion. Since the most significant features about the data are dominated by only some transform components, removing the redundancy of the data will be possible; 2) Since $Y = TX$, the transform domain covariance Σ_y is expressed by

$$\Sigma_y = T\Sigma_x T^{-1} = T\Sigma_x T^* \quad (33)$$

where T consists of the eigenvectors of Σ_x, which yields

$$\Sigma_y = \begin{bmatrix} \lambda_1 & & \\ & \ddots & \\ & & \lambda_N \end{bmatrix}. \quad (34)$$

This implies that the vector Y is unitary and uncorrelated.

Since the eigenvalues are the main diagonal terms of Σ_y, they correspond to the variances of the transform components $y^{(i)}$, $i = 1, \cdots, N$. Thus a logical criterion for selecting transform components is to retain the set of components with the M largest variance, while the remaining $(N - M)$ components are discarded. This process of components selection is referred to as the *variance criterion* method. Since the total variance of X is the sum of all eigenvalues of Σ_x, the variance-loss-ratio is defined by

$$\text{VLR} = \frac{\text{mean-square error}}{\text{total variance}} \times 100\%; \quad (35)$$

where the mean-square error is caused by eliminating some vectors. The compression-ratio is defined as

$$\text{CR} = \frac{\text{no. of vectors eliminated}}{\text{total no. of vectors}} \times 100\%. \quad (36)$$

These two ratios are used as the important performance indexes to test the effectiveness of the unitary compression.

B. Experimental Results

The experimental setup was as described in Section II, and the experimental conditions and parameters are same as these given previously. The test object, a metallized

100 : 1 scale model of B-52 aircraft, is mounted on a computer-controlled position situated in the anechoic chamber. The received Fourier space slice data is composed of 128 views spanning 90 degress rotation of the test object (i.e., 128 equally spaced views spanning a 90 degrees angular window), and 201 sampling points for each view covering a 2–17 GHz frequency bandwidth. Therefore, the measured scattering data set for the target is a 128 × 201 matrix representing 128 aspect views, each of which has 201 sampling points. The covariance representing the correlations between aspect views, can be formed for the 128 aspect views. Since the scattering data are of complex numbers, the covariance can be given by

$$\Sigma_x^{ij} = \frac{1}{N_{\text{samp}} - 1} \sum_{k=1}^{N_{\text{samp}}} (x_k^{(i)} - m_x^{(i)})(x_k^{(j)} - m_x^{(j)})^*; \tag{37}$$

where * denotes the complex transpose, N_{samp} denotes the number of the sampling points, and $m_x^{(i)}$ is the mean of $x^{(i)}$, which is computed as

$$m_x^{(i)} = \frac{1}{N_{\text{samp}}} \sum_{k=1}^{N_{\text{samp}}} x_k^{(i)} \qquad (i = 1, \cdots, N_{\text{view}}) \tag{38}$$

where N_{view} denotes the number of the aspect views. The covariance matrix Σ_x^{ij} is Hermitian and takes a maximum value when $i = j$. Both eigenvalues and eigenvectors of the covariance matrix are computed by using IMSL, a popular Fortran library for mathematical applications [19]. The Fourier space slice data received is transformed by the KLT which consists of the eigenvectors of the data's covariance and the data in transform domain are unitary, or uncorrelated with respect to each other. The eigenvalues solved by

$$\Sigma_x \phi_i = \lambda_i \phi_i \tag{39}$$

are illustrated in Fig. 4, where the eigenvalues, because of Hermitian nature of the covariance matrix, are real valued and can be ranked by magnitude. Since the eigenvalues are the main diagonal terms of Σ_y, they correspond to the variance of the transform component $y^{(i)}$. Thus, Fig. 4 will be referred to as the variance distribution. The area under the variance distribution curve for a given number of transform components is an indication of the amount of energy contained in those components. It is apparent that almost all of the signal energy (i.e., area under the curve) is packed into first half or one-third KLT components. Therefore, the most important information needed for image reconstruction is concentrated in only a few dominating aspect views and there is a great deal of redundancy in the raw data. According to *variance criterion*, these transform components corresponding to the larger eigenvalues contain the most significant features and should be kept, while the remaining with respect to smaller eigenvalues are considered as the redundant ones and discarded. The mean-square error caused by eliminating the redundant data can be minimized by discarding these aspects views with smaller associated eigenvalues.

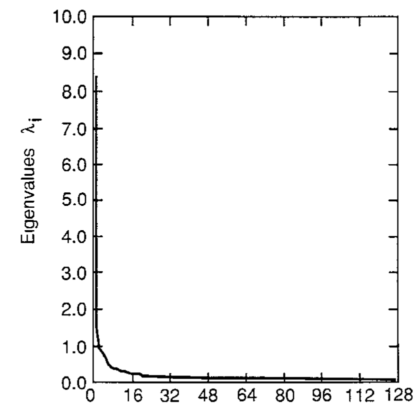

Fig. 4. Ordered eigenvalues of data's covariance.

TABLE I
VARIANCE-LOSS-RATIO (VLR) VERSUS COMPRESSION RATIO (CR)

CR (%)	VLR (%)
$\frac{10}{128} \approx 7.8\%$	.01%
$\frac{50}{128} \approx 39\%$	1%
$\frac{64}{128} \approx 50\%$	.15%
$\frac{100}{128} \approx 78\%$	4%
$\frac{120}{128} \approx 94\%$	18.6%

The relation between VLR and CR (both defined above) is demonstrated in Table I, where it is seen that, even when 64 vectors (half of the total number) are eliminated, the loss (i.e., mean-square error) is small, VLR = $\frac{1}{1000}$. If the signal energy is essentially contained in 43 of the 128 KLT components, a 3 : 1 data compression is considered. For a 3 : 1 compression, 43 KLT components corresponding to the largest diagonal terms of Σ_x are selected. Such a compressed unitary data set is denoted by $\hat{Y}$. An inverse KLT which, because of its unitary, is a complex transpose of T, is employed to reconstruct the image. Thus, the data to be used for image reconstruction are $\hat{X} = T * \hat{Y}$. The images reconstructed by employing unitary compression are presented in Figs. 5 and 6. As illustrated in Fig. 5 where half of the coordinates $y^{(i)}$ (64) are discarded, the reconstructed image is still legible and has same centimeter resolution as the original one shown in Fig. 1(a). Fig. 6 shows the reconstructed image when 2/3 of the received data have been discarded, i.e., a 3 : 1 data compression is achieved, in order to demonstrate that the centimeter resolution can be preserved. It is apparently shown in Fig. 6 that two engines on the wing can still be recognized, although there is some blurring. In conclusion, the unitary compression is an effective technique for dimension reduction in image reconstruction. It presents the statistical optimal solution for the data compression and feature extraction in the sense of minimizing the mean-square error. The *variance criterion* has

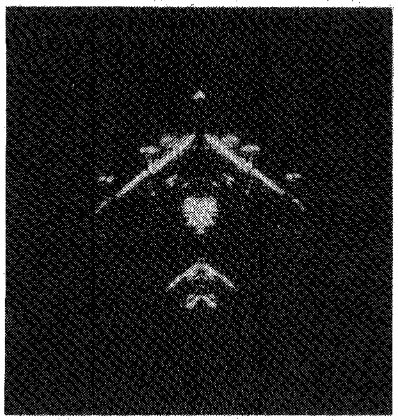

Fig. 5. Result of image with UCT when CR = 1/2 (half of the data are compressed).

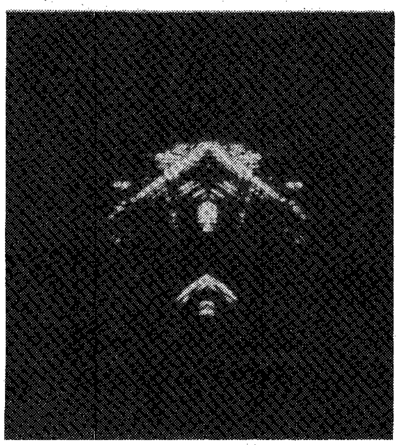

Fig. 6. Result of image with UCT when CR = 2/3 (two thirds' of the data are compressed).

demonstrated the capability of identifying the redundancy of the correlated data sets.

V. Conclusion

This work was initiated to study the feasibility of applying unitary compression to tomographic microwave diversity image reconstruction. It was found that a unitary transform, the Karhunen–Loéve transform, can provide a good representation of the data so that the redundancy of the data can be identified and thus allows for removal. This representation is based on minimizing the mean-square error, which leads to a statistical optimal solution. The mean-square error caused by discarding the redundant data is derived as the sum of those eigenvalues corresponding to the discarded data. Therefore, the eigenvalues of the data's covariance matrix are used as features to identify the redundancy of the data. According to the *variance criterion*, the discarded data, which is considered redundant, should be these with the smaller eigenvalues. The reconstructed images employing the unitary compression show that image quality is basicallly preserved after half of the total data has been selectively eliminated; and one can still identify most of details of the test model even when two-third's data are discarded. Although KLT is the optimal solution for unitary data compression, there are no fast computational algorithms since it involves solving the eigenvalues and eigenvectors of the data's covariance matrix. One is tempted, therefore, to employ suboptimal unitary transforms that possess fast computational algorithms. Discrete cosine transform (DCT) will be considered as an alternative unitary transformation for unitary compression. The performance evaluation of the effectiveness of unitary transforms will be studied in terms of rate-distortion function as a performance measure.

Targets can be identified either by reconstructing images with sufficient resolution to be recognized by a human observer, or by extracting features of the target for automated machine recognition. In future work, we will explore the use of unitary compression transform in neuromorphic target recognition. The unitary compression transform is used then as a feature detector in which the principal component can be extracted from the eigenvalues of the data's covariance matrix. The feature extraction based on the principal component method is by self-organization as shown in Oja's work [19]. Moreover, the unitary compression should be more effective when it is applied to target recognition, since it is expected that there is more redundancy in the data for this task than when the data are used for image reconstruction.

Acknowledgment

The authors would like to thank J. Tuazon for his help in carrying out some of the programming necessary to this project.

References

[1] N. H. Farhat, "Principles of broad-band coherent imaging," *J. Opt. Soc. Am.*, vol. 67, pp. 1015–1020, Aug. 1977.
[2] C. K. Chan and N. H. Farhat, "Frequency swept imaging of three dimensional perfectly reflecting objects," *IEEE Trans. Antennas Propagat.*, Special issues on Inverse scattering, vol. AP-29, pp. 312–319, Mar. 1981.
[3] N. H. Farhat, C. L. Werner, and T. H. Chu, "Prospects for three-dimensional projective and tomographic imaging radar network," *Radio Sci.*, vol. 19, pp. 1347–1355, Sept.-Oct. 1984.
[4] N. H. Farhat, "Microwave diversity imaging and automated target identification based on models of neural networks," *Proc. IEEE*, vol. 77, pp. 670–681, May 1989.
[5] E. L. Hall, *Computer Image Processing and Recognition.* New York: Academic, 1979.
[6] L. R. Rabiner and B. Gold, *Theory and Application of Digital Signal Processing.* Englewood Cliffs, NJ: Prentice-Hall, Inc., 1975.
[7] N. Bojarski, "Three-dimensional short pulse inverse scattering," *Syracuse Univ. Res. Rep.*, Syracuse, NY, 1967.
[8] R. M. Lewis, "Physical optics inverse diffraction," *IEEE Trans. Antennas Propagat*, vol. AP-17, pp. 308–314, May 1989.
[9] N. Ahmed and K. R. Rao, *Orthogonal Transforms for Digital Signal Processing.* New York: Springer-Verlag, 1975.
[10] M. Schwartz, *Information Transmission, Modulation, and Noise*, 3d edition. New York: McGraw-Hill, 1980.
[11] H. L. Van Trees, *Detection, Estimation, and Modulation Theory - Part I.* New York: Wiley, 1968.
[12] J. B. Burl, "Estimating the basis functions of the Karhunen-Loéve transform," *IEEE Trans. Acoust., Speech, and Sig. Proc.*, vol. 37, pp. 99–105, Jan. 1989.
[13] S. Watanabe, *Pattern Recognition: Human and Mechanical.* New York: Wiley 1985.

[14] K. Hoffman and R. Kunze, *Linear Algebra*, 2d ed. Englewood Cliffs, NJ: Prentice-Hall, 1971.
[15] I. N. Herstein, *Topics in Algebra*, 2d ed. New York: Wiley, 1975.
[16] S. Watanabe, "Karhunen-Loéve expansion and factor analysis," in *Proc. Trans. Fourth Prague Conf. Inform. Theory*, 1965.
[17] T. W. Anderson, *An Introduction to Multivariate Statistical Analysis*. New York: Wiley, 1958.
[18] E. Oja, "A Simplified Neuron Model as a Principal Component Analyzer," *J. of Math. Bio.*, vol. 15, pp. 267–273.
[19] IMSL MATH/LIBRARY - FORTRAN Subroutines for Mathematical Applications, Version 1.0, 1987.

Zijun Zhao (S'88–M'90) received the Ph.D. degree in electrical engineering from the Academia Sinica in 1986 and the M.A. degree in mathematics from the Temple University, Philadelphia, in 1987.

From 1988 to 1990 he was a Postdoctoral Fellow in the Moore School of Electrical Engineering at the University of Pennsylvania, and since 1990 he has been employed as a Research Associate at Penn, where he has been engaged in the research and development of digital and optic signal processing, compression and coding, photonic implementation of neural networks, and RF/microwave system design and imaging. His past research included optimal and stochastic control theory, synthetic aperture radar, DSP microprocessor embedded systems and telecommunication.

Dr. Zhao is a member of the Optical Society of America, the Society for Industrial and Applied Mathematics, and the American Society for the Advancement of the Sciences. He has been selected on the list of 1991 Marquis Who's Who in the East.

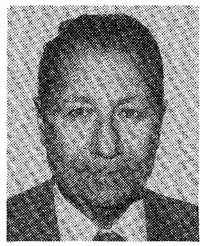

Nabil H. Farhat (S'58–M'63–SM'72–F'81) received the B.Sc. degree from the Technion Haifa, Israel in 1957, the M.Sc. degree from the University of Tennessee, Knoxville, in 1959, and the Ph.D. degree from the University of Pennsylvania, Philadelphia, in 1963, all in electrical engineering.

In 1964 he joined the Faculty of the Moore School of Electrical Engineering, University of Pennsylvania, where he is now Professor of Electrical Engineering and heads the Electro-Optics and Microwave-Optics Laboratory. His current research interests are in collective nonlinear dynamical information processing in neural networks and self-organizing systems, image understanding, microwave imaging and holography, optical information processing and photonic realization of neurocomputers in all of which he has numerous publications. His teaching includes courses in EM theory, electro-optics, electron and light optics, holography and neurodynamics on both graduate and undergraduate levels. His past research included the study of the interaction of EM radiation with plasmas and solids in the context of laser output energy measurement and photodetachment of negative ions.

While Associate Professor, he was named to the Ennis Chair in Electrical Engineering. In 1985 he was named Distinguished Visiting Scientist at the Jet Propulsion Laboratory, Pasadena, CA and has served in that capacity for several summers since then. He is a recipient of the University of Pennsylvania Christian R. and Mary F. Lindback Foundation award for distinguished teaching and is a Fellow of the Institute of Electrical and Electronics Engineers, and the Optical Society of America, and member of Sigma Xi, Eta Kappa Nu, the Electromagnetics Academy, and American Institute of Physics, the American Society for the Advancement of Science, and the American Institute of Physics, and has served on the National Board of Directors of Eta Kappa Nu and has been an RCA consultant since 1969. He has served as Editor of Advances in Holography and Associate Editor of Acoustical Imaging and Holography. He is presently action editor for two neural network journals: *Neural Networks* and *Neural Computation*.